

Local Time-Reversal Symmetry Breaking in $d_{x^2-y^2}$ Superconductors

M. J. Graf¹, A. V. Balatsky^{1,2}, and J. A. Sauls³

¹*Center for Materials Science, ²Theory Division*

Los Alamos National Laboratory, Los Alamos, New Mexico 87545

³*Department of Physics & Astronomy, Northwestern University, Evanston, Illinois 60208*

(April 18, 2018)

We show that an isolated impurity in a spin singlet $d_{x^2-y^2}$ superconductor generates a d_{xy} order parameter with locally broken time-reversal symmetry. The origin of this effect is a coupling between the $d_{x^2-y^2}$ and the d_{xy} order parameter induced by spin-orbit scattering off the impurity. The signature of locally broken time-reversal symmetry is an induced orbital charge current near the impurity, which generates a localized magnetic field in the vicinity of the impurity. We present a microscopic theory for the impurity induced d_{xy} component, discuss its spatial structure as well as the pattern of induced current and local magnetic field near the localized impurity spin.

PACS numbers: 74.25Bt, 74.62Dh

LA-UR: 99-1349

There is now strong evidence to support the identification of the superconducting state of many of the high T_c cuprates with a spin-singlet pairing amplitude having “d-wave” orbital symmetry, or more precisely $d_{x^2-y^2}$ symmetry.¹ This phase preserves time-reversal (\mathcal{T}) symmetry, but changes sign under reflection along the $[110]$ and $[\bar{1}10]$ mirror planes, as well as $\pi/2$ -rotations in a tetragonal crystal. As a consequence $d_{x^2-y^2}$ pairing correlations are particularly sensitive to scattering of quasiparticles on the Fermi surface. In this article we show that an isolated impurity in a spin singlet $d_{x^2-y^2}$ superconductor generates a complex d_{xy} order parameter (OP) with locally broken \mathcal{T} symmetry; the signature of this effect is an induced orbital charge current near the impurity and a localized magnetic field in the vicinity of the impurity.

Atomic scale impurities, or defects, scatter conduction electrons which leads to local suppression of the superconducting OP (pair-breaking) near the impurity. The mechanism responsible for pair-breaking is the formation of quasiparticle states near the Fermi level which are bound to the impurity by Andreev scattering.² The corresponding reduction in the spectral weight of the pair condensate is responsible for pair-breaking. The existence of quasiparticle states near the Fermi level can also lead to local Fermi-surface instabilities and mixing of order parameters with different symmetry.³ Low temperature phase transitions associated with a secondary OP may provide new information on the mechanism(s) for pairing in unconventional superconductors,⁴ while impurity-induced *mixing* of the $d_{x^2-y^2}$ OP with an OP of different symmetry can provide direct information on the atomic structure of the impurity.⁵

Recent transport experiments report evidence for low temperature phases associated with a secondary OP at surfaces ($T_s \simeq 8$ K).⁶ This was interpreted in terms of a surface phase transition to a $d_{x^2-y^2} + is$ state with spontaneously broken \mathcal{T} -symmetry.⁴ Bulk transport measurements on $\text{Bi}_2\text{Sr}_2\text{CaCu}_2\text{O}_{8+\delta}$ (Bi-2212) show a

pronounced drop in the thermal conductivity at $T^* \approx 150$ mK $\ll T_c \approx 80$ K in Ni doped Bi-2212.⁷ This anomaly was interpreted as the signature of a second superconducting phase with a fully gapped quasiparticle spectrum and a mixed symmetry OP of the form $d_{x^2-y^2} + id_{xy}$. This phase was proposed to arise from a coupling of the orbital momentum of the conduction electron with the spin of the magnetic impurity, $\mathcal{H}_{so} = \int d\mathbf{r} \psi_\alpha^\dagger(\mathbf{r}) v(r) \mathbf{L}_{\text{orbit}} \cdot \mathbf{S}_{\text{imp}} \psi_\alpha(\mathbf{r})$.⁵ Measurements of the spin-orbit coupling energy for Ni^{2+} ions indicate that it is a few percent of the nonmagnetic and exchange channels.⁸ In this model the id_{xy} OP is induced at a temperature above the second phase transition, $T^* < T \leq T_c$; the low temperature transition is argued to be ordering of the impurity-induced “patches” of the local $d_{x^2-y^2} \pm id_{xy}$ order.⁵ Above T^* patches with randomly fluctuating internal phase destroy the long range order, $\langle d_{xy} \rangle = 0$, but preserve $\langle |d_{xy}|^2 \rangle \neq 0$. Thus, the local structure associated with $d_{x^2-y^2} \pm id_{xy}$ symmetry near a magnetic impurity should be observable at temperatures well above T^* . The electronic and magnetic structure near an impurity located near the surface of a superconductor can now be studied with atomic resolution at low temperature by scanning tunneling microscopy (STM), opening a new window for local probes.^{9,10}

In this article we investigate theoretically the local structure of the OP and the current distribution in the neighborhood of an atomic impurity within the $d_{x^2-y^2}$ model for the high T_c cuprates. We present new analytical and numerical results for the local $d_{x^2-y^2} \pm id_{xy}$ OP that develops near a magnetic impurity, which has attracted new theoretical interests.^{11,12} Our approach follows closely the theory developed in the late 70’s for ions in superfluid ^3He ,^{13,2} and later adapted to study the properties of impurities in heavy fermion superconductors.^{14,15} The theory of impurity scattering in superconductors can be formulated to quasiclassical accuracy as an expansion in σ/ξ_0 , where σ is the (linear in 2D) cross-section of the impurity for scattering

of normal-state quasiparticles at the Fermi surface, and $\xi_0 = v_f/\pi\Delta_0$ is the superconducting coherence length. This ratio is typically very small in low T_c superconductors and in superfluid ^3He , but may be as big as 0.2 for strong scatterers in high T_c superconductors.

We start from Eilenberger's transport equation, for the matrix propagator in particle-hole/spin space, $\hat{g}(\mathbf{p}_f, \mathbf{r}; \epsilon_n)$. The diagonal element of the propagator determines the local density of states and local equilibrium current distribution, and the off-diagonal elements are the components of the local pair amplitude. Quasiparticle scattering off an isolated impurity is included through a *source* term on the *r.h.s* of the Eilenberger equation.² The transport equation can be linearized to leading order in σ/ξ_0 for distances $r \gg \sigma$ from the impurity. In this limit the Fourier transform of the linearized transport equation reduces to,¹⁵

$$[i\epsilon_n \hat{\tau}_3 - \hat{\Delta}_b - \hat{\sigma}_{\text{imp}}, \delta \hat{g}] + \mathbf{q} \cdot \mathbf{v}_f \delta \hat{g} = [\hat{t} + \delta \hat{\Delta} + \delta \hat{\sigma}_{\text{imp}}, \hat{g}_b]. \quad (1)$$

The bulk propagator, $\hat{g}_b(\mathbf{p}_f; \epsilon_n) = -\pi[i\tilde{\epsilon}_n \hat{\tau}_3 - \hat{\Delta}_b(\mathbf{p}_f)]/E$, order parameter, $\hat{\Delta}_b(\mathbf{p}_f) = \Delta_b(\mathbf{p}_f) \hat{\tau}_1 i\sigma_2$, impurity scattering self-energy, $\hat{\sigma}_{\text{imp}}$, and in-plane Fermi velocity, \mathbf{v}_f , are inputs to the linear response equations. The energy denominator is given by $E = (|\Delta_b(\mathbf{p}_f)|^2 + \tilde{\epsilon}_n^2)^{1/2}$, where $\tilde{\epsilon}_n = \epsilon_n + \frac{i}{4} \text{Tr} \hat{\tau}_3 \hat{\sigma}_{\text{imp}}(\epsilon_n)$ is the renormalized Matsubara frequency. The \hat{t} matrix for the isolated impurity, as well as the induced OP, $\delta \hat{\Delta} = [\delta \Delta_1 \hat{\tau}_1 + \delta \Delta_2 \hat{\tau}_2] i\sigma_2$, and self-energy, $\delta \hat{\sigma}_{\text{imp}}$, enter the *r.h.s* of Eq. (1) as source terms. Here $\hat{\tau}_i$ and σ_i are Pauli matrices in particle-hole and spin space, respectively. The \hat{t} matrix for the isolated impurity is given by

$$\begin{aligned} \hat{t}(\mathbf{p}_f, \mathbf{p}'_f; \epsilon_n) &= \hat{v}(\mathbf{p}_f, \mathbf{p}'_f) + N_f \int d^2 \mathbf{p}''_f \hat{v}(\mathbf{p}_f, \mathbf{p}''_f) \\ &\quad \times \hat{g}_b(\mathbf{p}''_f; \epsilon_n) \hat{t}(\mathbf{p}''_f, \mathbf{p}'_f; \epsilon_n), \end{aligned} \quad (2)$$

where N_f is the 2D density of states at the Fermi energy per spin, and $\hat{v}(\mathbf{p}_f, \mathbf{p}'_f)$ is the impurity potential, which is evaluated in the forward scattering limit in Eq. (1); $\mathbf{p}'_f = \mathbf{p}_f$. We separate \hat{v} into channels for nonmagnetic (u), spin-spin exchange ($\mathbf{m} = J\mathbf{S}_{\text{imp}}$), and spin-orbit scattering (\mathbf{u}_{so}) between the orbital momentum of the quasiparticle and the impurity spin, \mathbf{S}_{imp} , as well as the self-coupling (\mathbf{w}_{so}) to the quasiparticle spin, $\hat{\mathbf{S}}$,^{16,17}

$$\begin{aligned} \hat{v}(\mathbf{p}_f, \mathbf{p}'_f) &= u(\mathbf{p}_f, \mathbf{p}'_f) + \mathbf{m}(\mathbf{p}_f, \mathbf{p}'_f) \cdot \hat{\mathbf{S}} + \\ &\quad i[\mathbf{u}_{\text{so}}(\mathbf{p}_f, \mathbf{p}'_f) \cdot \mathbf{S}_{\text{imp}} + \mathbf{w}_{\text{so}}(\mathbf{p}_f, \mathbf{p}'_f) \cdot \hat{\mathbf{S}}] \hat{\tau}_3. \end{aligned} \quad (3)$$

The induced OP is self-consistently determined from the gap equation,

$$\delta \hat{\Delta}(\mathbf{p}_f, \mathbf{q}) = N_f T \sum_{\epsilon_n} \int d^2 \mathbf{p}'_f V(\mathbf{p}_f, \mathbf{p}'_f) \hat{f}(\mathbf{p}'_f, \mathbf{q}; \epsilon_n), \quad (4)$$

where $V(\mathbf{p}_f, \mathbf{p}'_f)$ is the pairing interaction and $\hat{f} = [\delta f_1 \hat{\tau}_1 + \delta f_2 \hat{\tau}_2] i\sigma_2$ is the induced off-diagonal pair amplitude. We resolve the pairing interaction into the dominant attractive $d_{x^2-y^2}$ channel, and a secondary pairing channel with d_{xy} symmetry, $V(\mathbf{p}_f, \mathbf{p}'_f) = V_1 \eta_1(\phi) \eta_1(\phi') +$

$V_2 \eta_2(\phi) \eta_2(\phi')$, where the eigenfunctions are $\eta_1(\phi) = \cos 2\phi$ and $\eta_2(\phi) = \sin 2\phi$ for the two channels, respectively. The dominant, attractive interaction is $V_1 \equiv V_{x^2-y^2}$, and the subdominant interaction, $V_2 \equiv V_{xy}$, may be either attractive or repulsive. We neglect the s -wave pairing channel in order to simplify the analysis, and we restrict our discussion to the regime in which the subdominant interaction, V_{xy} , is repulsive or too weak to nucleate a bulk d_{xy} OP.

Numerical calculations of the OP and current distribution were carried out for an isolated impurity at $\mathbf{r} = 0$, with the \hat{t} matrix source term of the form $\hat{t}(\mathbf{p}_f, \mathbf{p}_f; \epsilon_n) \delta(\mathbf{r})$ in real space. We modeled the position of the impurity to quasiclassical accuracy by replacing the delta function by a smooth function, $\delta_{r_0}(\mathbf{r}) = \frac{1}{\pi r_0^2} \exp(-r^2/r_0^2)$, of atomic width $r_0 = 0.1\xi_0$. This model guarantees a smooth cutoff in \mathbf{q} -space and faster convergence of the Fourier integrals. For the computation reported here we also chose a subdominant pairing interaction corresponding to a bare subdominant transition temperature of $T_{c2}/T_{c1} = 0.1$, which is well below the threshold for bulk nucleation of a d_{xy} order parameter.

The physical solution to the linearized transport equation (1) is,¹⁵

$$\delta \hat{g}(\mathbf{p}_f, \mathbf{q}; \epsilon_n) = \frac{E \hat{g}_b + \pi Q}{2\pi(E^2 + Q^2)} [\hat{t} + \delta \hat{\Delta} + \delta \hat{\sigma}_{\text{imp}}, \hat{g}_b], \quad (5)$$

where $Q = \frac{1}{2} \mathbf{q} \cdot \mathbf{v}_f$. The induced charge current is also determined by the \hat{t} matrix and induced OP,

$$\delta \mathbf{j}(\mathbf{q}) = N_f T \sum_{\epsilon_n} \int d^2 \mathbf{p}_f \mathbf{v}_f \frac{2i\pi e Q \Delta_1}{E(E^2 + Q^2)} (t_2 + \delta \Delta_2), \quad (6)$$

where t_2 is the $\hat{\tau}_2$ component of \hat{t} .

We evaluate the \hat{t} matrix in second-order Born approximation, which is adequate for weak scattering. More importantly, the Born approximation generates the relevant coupling between the $d_{x^2-y^2}$ and d_{xy} order parameters. We also assume that the impurity potential is short-ranged, so we retain only the scattering amplitudes for the s -wave and p -wave channels, *i.e.*, $u(\mathbf{p}_f, \mathbf{p}'_f) \approx u_0 + u_1 \mathbf{p}_f \cdot \mathbf{p}'_f$, and $\mathbf{m}(\mathbf{p}_f, \mathbf{p}'_f) \approx (J_0 + J_1 \mathbf{p}_f \cdot \mathbf{p}'_f) \mathbf{S}_{\text{imp}}$. For the spin-orbit terms we approximate, $\mathbf{u}_{\text{so}}(\mathbf{p}_f, \mathbf{p}'_f) \approx (\lambda_0 + \lambda_1 \mathbf{p}_f \cdot \mathbf{p}'_f) \mathbf{p}_f \times \mathbf{p}'_f$, and $\mathbf{w}_{\text{so}}(\mathbf{p}_f, \mathbf{p}'_f) \approx (w_0 + w_1 \mathbf{p}_f \cdot \mathbf{p}'_f) \mathbf{p}_f \times \mathbf{p}'_f$. The \hat{t} matrix then has the general form $\hat{t} = [t_1 \eta_1 \hat{\tau}_1 + t_2 \eta_2 \hat{\tau}_2] i\sigma_2 + [t_3 + \mathbf{t} \cdot \hat{\mathbf{S}}] \hat{\tau}_3$. The important interference term is given by

$$t_2(\epsilon_n) = \pi S_z N_f \tilde{\lambda}^2 \int \frac{d\phi}{2\pi} \frac{\Delta_1 \eta_1^2(\phi)}{\sqrt{|\Delta_1 \eta_1(\phi)|^2 + \tilde{\epsilon}_n^2}}, \quad (7)$$

with the spin-orbit parameter $\tilde{\lambda}^2 = u_0 \lambda_1 + u_1 \lambda_0 + J_0 w_1 + J_1 w_0$, and the impurity spin S_z . The t_2 term generates a correction to the off-diagonal propagator with $d_{x^2-y^2}$ (B_{1g}) symmetry and induces the id_{xy} (B_{2g}) OP near the impurity.

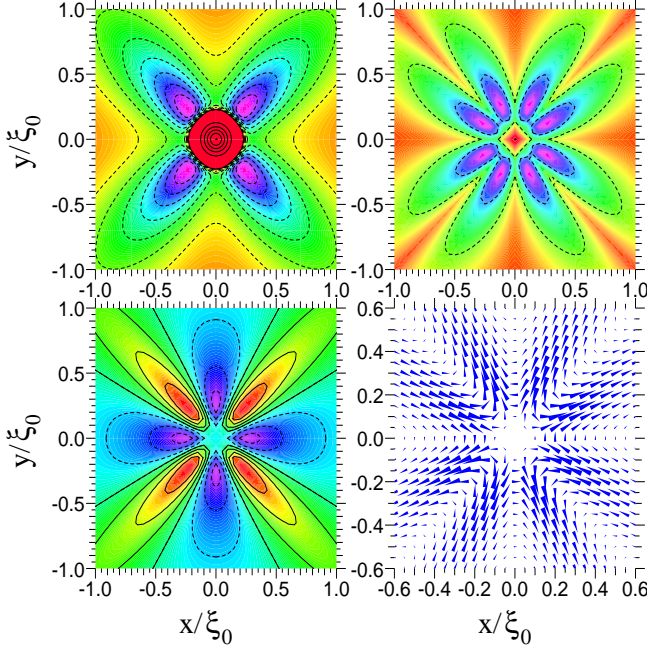


FIG. 1. Contour plots of the induced id_{xy} OP (top left), the current density (top right), and the magnetic field (bottom left), at $T = 0.1T_c$ for $T_{c2}/T_{c1} = 0.1$ with no bulk scatterers. Solid (dashed) lines are negative (positive) contour lines. Bottom right: Field plot of the current density.

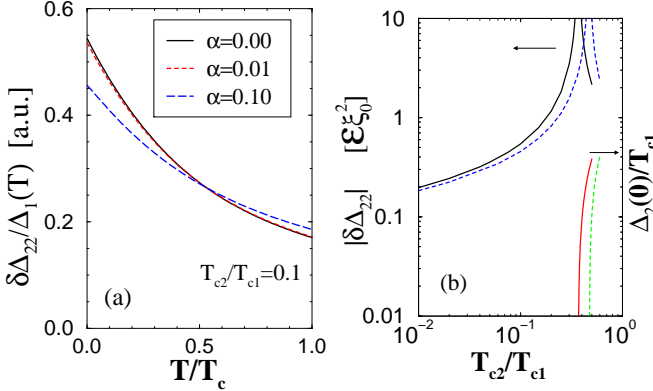


FIG. 2. Induced id_{xy} OP at $\mathbf{q} = 0$. (a) $\delta\Delta_{22}$ normalized by the $\Delta_1(T)$ OP vs. $T_c = T_c(\alpha)$ for different bulk scattering rates $\alpha = 1/(2\pi T_{c1}\tau)$. (b) $\delta\Delta_{22}$ and the bulk Δ_2 OP for attractive pairing potentials (T_{c2}/T_{c1}) at $T = 0$ for $\alpha = 0.0$ (solid) and $\alpha = 0.1$ (dashed). See text for the definition of \mathcal{E} .

The corrections to the bulk OP, $\delta\Delta_i$, with $i = 1, 2$, do not belong to a single representation, *i.e.*, $\delta\Delta_i(\phi, \mathbf{q}) \not\propto \eta_i(\phi)$. In particular, $\delta\Delta_2(\phi, \mathbf{q})$ has mixed d_{xy} and $d_{x^2-y^2}$ symmetry, $\delta\Delta_2(\phi, \mathbf{q}) = \delta\Delta_{21}(\mathbf{q})\eta_1(\phi) + \delta\Delta_{22}(\mathbf{q})\eta_2(\phi)$. These amplitudes also determine the current distribution (6), and satisfy the coupled equations

$$[1/V_1 - \mathcal{K}_{11}(\mathbf{q})]\delta\Delta_{21}(\mathbf{q}) - \mathcal{K}_{12}\delta\Delta_{22}(\mathbf{q}) = \mathcal{A}_1(\mathbf{q}), \quad (8)$$

$$[1/V_2 - \mathcal{K}_{22}(\mathbf{q})]\delta\Delta_{22}(\mathbf{q}) - \mathcal{K}_{12}\delta\Delta_{21}(\mathbf{q}) = \mathcal{A}_2(\mathbf{q}), \quad (9)$$

where $\mathcal{K}_{ij}(\mathbf{q}) = \pi T \sum_{\epsilon_n} \int \frac{d\phi}{2\pi} \eta_i(\phi) \eta_j(\phi) E / [E^2 + Q^2]$, and $\mathcal{A}_i(\mathbf{q}) = \pi T \sum_{\epsilon_n} t_2(\epsilon_n) \int \frac{d\phi}{2\pi} \eta_i(\phi) \eta_2(\phi) E / [E^2 + Q^2]$. The solutions to these equations have, in addition to inversion symmetry, the mirror reflections $\delta\Delta_{2i}(q_1, q_2) =$

$(-)^i \delta\Delta_{2i}(q_1, -q_2) = (-)^i \delta\Delta_{2i}(q_2, q_1)$. The induced $\delta\Delta_{22}$ OP component with B_{2g} symmetry is finite for $\mathbf{q} = 0$, while the induced $\delta\Delta_{21}$ component with B_{1g} symmetry vanishes for $\mathbf{q} = 0$ and along the diagonals and principle axes. The Fourier transformation of $\delta\Delta_{21}(\mathbf{q})$ also vanishes, *i.e.*, $\delta\Delta_{21}(\mathbf{r}) = 0$; thus only the induced component with B_{2g} symmetry survives. The contour plot of $\delta\Delta_2(\mathbf{r})$ in Fig. 1 shows a four-fold pattern characteristic of the d_{xy} amplitude with maxima located at approximately $0.3\xi_0$ along the nodal directions of the $d_{x^2-y^2}$ OP.

Bulk impurity scattering is pair-breaking for any unconventional OP including the induced d_{xy} amplitude. Figure 2 shows both the temperature dependence of the induced d_{xy} OP and the pair-breaking suppression of $\delta\Delta_{22}(\mathbf{q} = 0)$ by bulk impurity scattering. Note that the d_{xy} OP develops below T_c and that it is suppressed by bulk scattering on the same scale as the bulk $d_{x^2-y^2}$ OP. Fig. 2(b) shows the increase in the induced d_{xy} amplitude with increasing (attractive) pairing interaction in the B_{2g} channel (T_{c2}/T_{c1}); the divergence at $T_{c2}/T_{c1} > 0.37$ corresponds to a bulk instability for $d_{x^2-y^2} \pm id_{xy}$ pairing. For a repulsive pairing interaction $V_2 < 0$ we find a cutoff dependent result for the induced OP, $-0.44 \mathcal{E} \xi_0^2 / \log(\omega_c/\Delta_1) < \delta\Delta_{22}(q=0) < 0$, at $T = 0$. We parameterized the interference term in the scattering amplitude by the coupling energy $\mathcal{E} = \pi S_z N_f \lambda^2 / \xi_0^2$,

The existence of a $\pm id_{xy}$ OP implies that the equilibrium superconducting state breaks \mathcal{T} symmetry *locally* near the impurity, in addition to broken $[110]$ and $[100]$ reflection symmetries. The signature of the $d_{x^2-y^2} \pm id_{xy}$ state is the equilibrium charge current and magnetic field distribution near the impurity.^{13–15,18} From the \hat{t} matrix in Eq. (2) and the induced d_{xy} OP we obtain

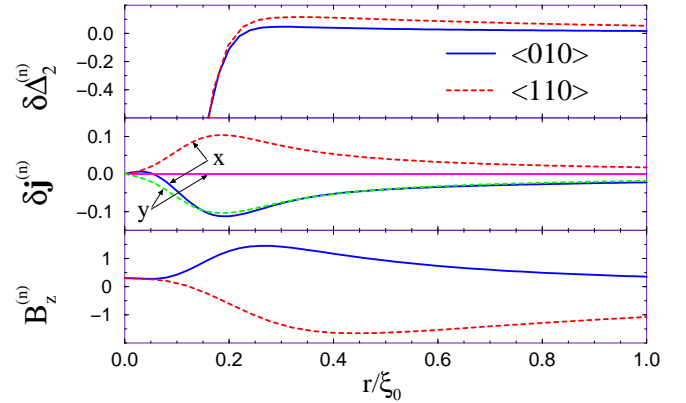


FIG. 3. Spatial dependence of the normalized OP, $\delta\Delta_2^{(n)}(\mathbf{r})$, current density, $\delta\mathbf{j}^{(n)}(\mathbf{r})$ (x and y components), and magnetic field, $B_z^{(n)}(\mathbf{r})$, along the $\langle 010 \rangle$ and $\langle 110 \rangle$ directions at $T = 0.1T_c$ for a modest d_{xy} pairing interaction of $T_{c2}/T_{c1} = 0.1$ (well below the bulk transition to $d_{x^2-y^2} + id_{xy}$).

$$\delta\mathbf{j}(\mathbf{q}) = i\pi e N_f T \sum_{\epsilon_n} \int \frac{d\phi}{2\pi} \mathbf{v}_f(\phi) \mathbf{v}_f(\phi) \cdot \mathbf{q} \frac{\Delta_1 \eta_1(\phi)}{E(E^2 + Q^2)} \times \left((t_2(\epsilon_n) + \delta\Delta_{22}(\mathbf{q}))\eta_2(\phi) + \delta\Delta_{21}(\mathbf{q})\eta_1(\phi) \right). \quad (10)$$

It is straightforward to show that the current density obeys the symmetry relations: $\delta\mathbf{j}(\mathbf{q}) = -\delta\mathbf{j}(-\mathbf{q})$,

and $\delta j_i(q_1, q_2) = (-)^{i+1} \delta j_i(-q_1, q_2)$, $\delta j_1(q_1, q_2) = -\delta j_2(q_2, q_1)$. From these relations one might expect a simple circulation pattern for the induced charge current; however, as Figs. 1 and 3 show, the current density exhibits the superposition of a very small circulating current loop and four counter circulating currents around the nodal directions, which are anchored to the local maxima of the induced $\delta\Delta_2(\mathbf{r})$ OP. This pattern is qualitatively similar to the current distribution predicted for a vortex with $d+is$ symmetry,¹⁹ however, there is no circulation at large distances from the impurity. The complex flow pattern that is observed near the impurity is also observed for mesoscopic superconductors with surfaces that are normal to the $\langle 110 \rangle$ direction,²⁰ and reflects the strong nonlocality of the current response shown in Eq. (10).

The spatial pattern of current generates a four-fold magnetic field distribution which we calculated from the current distribution using the Biot-Savart law, $B_z(\mathbf{r}) = \frac{1}{c} \int d^2\mathbf{r}' |\mathbf{r}' - \mathbf{r}|^{-3} (\mathbf{r}' - \mathbf{r}) \times \delta \mathbf{j}(\mathbf{r}')$. The field distribution in Fig. 1 shows 8 sectors of flux threading in and out of the plane. As a result the net magnetic flux through the superconducting plane is zero. This fact was checked numerically. The magnetic flux was calculated for squares of area L^2 and shown to vanish in the limit $L \rightarrow \infty$. This is a general result, at least at the quasiclassical level, provided that scattering by the impurity does not generate a coupling of the current to a soft mode of the OP.¹⁴ However, particle-hole asymmetry corrections to the quasiclassical theory may lead to a net moment from the impurity-induced orbital currents.

The magnitudes of the induced id_{xy} OP and magnetic field near an impurity depend on parameters characterizing the interaction between quasiparticles and the magnetic impurity. Not much is known about these interactions. Thus, measurements of the induced OP or magnetic field near an impurity can provide direct information about the coupling of the quasiparticle orbital momentum to the impurity moment. We can express the impurity induced OP, current density and magnetic field in terms of a few key material parameters of the impurity. We scale the induced OP in units of the coupling energy, $\delta\Delta_2^{(n)}(\mathbf{r}) = \delta\Delta_2(\mathbf{r})/\mathcal{E}$. From Eq. (10) we obtain the scale of the current and field: $\delta \mathbf{j}^{(n)}(\mathbf{r}) = \delta \mathbf{j}(\mathbf{r})/(c\mathcal{B})$, $B_z^{(n)}(\mathbf{r}) = B_z(\mathbf{r})/\mathcal{B}$, with $\mathcal{B} = \frac{e}{c} N_f v_f \mathcal{E} = \frac{\Phi_0}{4\pi\lambda^2} \frac{\mathcal{E}d}{\pi\hbar v_f}$. Figure 3 shows the spatial variations of the scaled OP, current density and field profile along the $\langle 110 \rangle$ and $\langle 010 \rangle$ directions at low temperature.

We estimate the magnitude of the induced OP and magnetic field for Ni impurities in Bi-2212 as follows: The coupling parameter for Ni^{2+} ions is estimated from the spin-orbit coupling energy for free Ni^{2+} ions,⁸ $\tilde{\lambda}^2 \sim (30 \text{ meV} \cdot a_0^2)^2$. The in-plane penetration depth of $\lambda \approx 200 \text{ nm}$, the interlayer spacing, $d \approx 1.5 \text{ nm}$, the in-plane lattice constant, $a_0 \approx 5.4 \text{ \AA}$, and the Fermi velocity, $v_f \sim 100 \text{ km/s}$, provide a determination of the density of states per Cu-O bilayer, $N_f = c^2 d / (4\pi e^2 v_f^2 \lambda^2)$. This gives an estimated energy scale for the induced d_{xy} gap of $\mathcal{E} \sim 0.1 \text{ meV}$, and a magnetic field scale of order

$\mathcal{B} \sim 1 \mu\text{T}$. An induced d_{xy} gap of order $0.1 \text{ meV} \approx 1 \text{ K}$, is the right order of magnitude to account for a $d_{x^2-y^2} \pm id_{xy}$ phase order transition at lower temperature, $T^* \sim 150 \text{ mK}$, as observed in 0.6% and 1.5% Ni doped Bi-2212.^{7,5}

In conclusion, we have shown that spin-orbit scattering induces a $d_{x^2-y^2} + id_{xy}$ state, which locally breaks \mathcal{T} symmetry in the vicinity of a magnetic impurity. The induced OP develops below T_c and survives bulk impurity scattering so long as the bulk $d_{x^2-y^2}$ OP does. The signature of the spontaneously broken \mathcal{T} symmetry manifests itself as a complex pattern of circulating charge currents near the local maxima of the d_{xy} OP located along the $\langle 110 \rangle$ and $\langle \bar{1}10 \rangle$ directions. We estimated the magnitude of the induced d_{xy} gap to be $\sim 1 \text{ K}$, which should be observable in low temperature STM measurements of the tunneling density of states.

We thank R. Movshovich, D. Rainer and J.R. Schrieffer for discussions. The work of MJG and AVB was supported by the Los Alamos National Laboratory under the auspices of the US Department of Energy. JAS acknowledges support by the STCS through NSF DMR-91-20000.

¹ D. Van Harlingen, Rev. Mod. Phys. **67**, 515 (1995).

² E. Thuneberg, J. Kurkijärvi, and D. Rainer, Physica **107B**, 43 (1981); J. Phys. C **14**, 5615 (1981).

³ L. J. Buchholtz, M. Palumbo, D. Rainer, and J. A. Sauls, J. Low Temp. Phys. **101**, 1099 (1995).

⁴ M. Fogelström, D. Rainer, and J. A. Sauls, Phys. Rev. Lett. **79**, 281 (1997).

⁵ A. V. Balatsky, Phys. Rev. Lett. **80**, 1972 (1998); A. V. Balatsky and R. Movshovich, J. Phys. Chem. Sol. **59**, 1689 (1998); Physica B **261**, 446 (1999).

⁶ M. Covington *et al.*, Phys. Rev. Lett. **79**, 277 (1997).

⁷ R. Movshovich *et al.*, Phys. Rev. Lett. **80**, 1968 (1998).

⁸ K. Yosida, *Theory of magnetism* (Springer, Berlin, 1996).

⁹ A. Yazdani *et al.*, Science **275**, 1767 (1997); e-print: cond-mat/9906001.

¹⁰ E. W. Hudson, S. H. Pan, A. K. Gupta, K-W Ng, and J. C. Davis (unpublished).

¹¹ C. Grimaldi, e-print: cond-mat/9905262.

¹² M. E. Simon and C. M. Varma, e-print: cond-mat/9905349.

¹³ D. Rainer and M. Vuorio, J. Phys. C **10**, 3093 (1977).

¹⁴ C. H. Choi and P. Muzikar, Phys. Rev. B **39**, 9664 (1989).

¹⁵ C. H. Choi and P. Muzikar, Phys. Rev. B **41**, 1812 (1990).

¹⁶ Y. S. Barash, A. G. Grishin, and M. Sigrist, JETP **85**, 168 (1997).

¹⁷ The spin operator of the conduction electrons is defined as $\hat{\mathbf{S}} = \frac{1}{2}(1 + \hat{\tau}_3)\boldsymbol{\sigma} - \frac{1}{2}(1 - \hat{\tau}_3)\sigma_2\boldsymbol{\sigma}\sigma_2$.

¹⁸ M. I. Salkola and J. R. Schrieffer, Phys. Rev. B **58**, R5952 (1998).

¹⁹ M. Franz *et al.*, Phys. Rev. B **53**, 5795 (1996).

²⁰ H. Burkhardt, J. A. Sauls, and D. Rainer, Bull. Am. Phys. Soc. **43**, 800 (1998).